



A comprehensive study on electronic structure and optical properties of carbon nanotubes with doped B, Al, Ga, Si, Ge, N, P and As and different diameters



İskender Muz ^{a,*}, Mustafa Kurban ^{b,**}

^a Department of Mathematics and Science Education, Nevşehir Hacı Bektaş Veli University, 50300, Nevşehir, Turkey

^b Department of Electronics and Automation, Ahi Evran University, 40100, Kırşehir, Turkey

ARTICLE INFO

Article history:

Received 26 March 2019
Received in revised form
14 June 2019
Accepted 17 June 2019
Available online 19 June 2019

Keywords:

Carbon nanotubes
Atom doping
Electronic structure
Chemical reactivity
DFT

ABSTRACT

Density functional theory (DFT) is used for investigating the electronic structure and optical properties carbon nanotubes (CNTs) with doped B, Al, Ga, Si, Ge, N, P and As and different diameters. Our results show that the stability of CNTs increased when it comes to an increase in diameter, however, stability decreases depending on doping additives to pure CNTs. B-doped CNTs are the most effective for electronic conductivity due to its lower band gap. The non-linear optical (NLO) properties are discussed according to dipole moment, polarizability, and hyperpolarizability. All the doped CNTs exhibit a good NLO activity. B-, Al-, Ga- and N-doped CNTs have a significant effect on NLO properties. The band gap of CNTs considerably decreased from 2.76 eV to 1.40 eV and 1.78 eV–0.83 eV based on the diameter. The reactivity properties investigated based on chemical hardness, softness, and potential, electronegativity, electrophilicity, the maximum amount of electronic charge index, the electron accepting and donating capability as well as electronic density of states are also presented and analyzed. Herein, the results indicated that the characteristic properties of CNTs can be controlled with different atoms doped CNTs and diameters.

© 2019 Elsevier B.V. All rights reserved.

1. Introduction

Recently, one dimensional (1D) materials have attracted considerable attention because of their wide range applications in different areas [1–4]. Among the 1D materials, in particular, carbon nanotubes (CNTs) have unique and tunable electronic and optical properties based on their size and morphology. Herein, considerable efforts regarding the study of properties and applications of CNTs have been dedicated by experimental and theoretical investigations in the recent years [5–8] to improve and control their properties. Among them, the studies of diameter and the types of doped single atom, such as boron (B), aluminum (Al), gallium (Ga), silicon (Si), germanium (Ge), nitrogen (N), and phosphorous (P) doped CNTs have been continuously investigated due to their interesting properties from both a fundamental physics and the

possible applications viewpoint. For example, CNTs have tunable thermal conductivity (κ) properties depending on the diameter [9]. Although several experiments have been carried out on κ values, it is still difficult to obtain a reasonable result because of diameter of CNTs [10,11]. Therefore, it is significant to clarify the relationship between CNT's characteristic parameters and diameters. On the other hand, doping of carbon-based nanomaterials with foreign atoms is an effective approach to modify the electronic properties and chemical activities for consequent tuning of their electrochemical properties [12,13], and thus doped CNTs have new desirable properties such as high activity and excellent stability [14–17]. The previous studies show that, B- or N-doped CNTs give rise to a decrease in the band gap of pure CNTs thus the doped CNT needs less energy cost [18,19]. The advances in the design of doped CNTs have shown that it is possible to enhance the conductivity of CNTs which means a rise of the number of holes which are charge carriers [20]. Moreover, N-doped CNT has a huge effect on the reducing O₂ and H₂ dissociation barriers on CNTs [21,22] and the facile oxygen reduction reaction [23,24]. The capability of absorption of gas molecules in nickel (Ni) and silicon (Si) doped CNTs is also more desirable than pure CNTs [25]. Si-doped CNT is also a good

* Corresponding author.

** Corresponding author.

E-mail addresses: iskendermuz@yahoo.com (İ. Muz), mkurbanphys@gmail.com (M. Kurban).

candidate for gas sensors or drug delivery devices because of its considerable impact on the reactivity of CNTs [26,27]. The performance of Al-doped CNTs have been exhibited for organic pollutant removal and anticancer drug cisplatin [28,29]. Ge- and P-doped CNTs have potential as a material with high electrocatalytic activity for oxygen reduction reaction and in other applications such as lithium-air batteries, photocatalysis, and heterocatalysis [30]. Ga-doped CNTs exhibit superior field emission property, which is much better than B- and N-doped as well as undoped CNTs [31].

In the literature, there is no systematic study on the electronic structure and optical properties of B-, Al-, Ga-, Si-, Ge-, N-, P- and As-doped CNTs with different diameters. In this study, we researched the binding energy, formation energy, total energy, chemical hardness and softness, chemical potential, HOMO-LUMO energy gap, density of state, refractive index, electronegativity, electrophilicity, maximum amount electronic charge index, ionization potential and electron affinity. Non-linear optical (NLO) behaviors were performed by analyzing the polarizability, and hyperpolarizability. All calculations were performed by quantum chemistry calculations.

2. Computational details

The $3 \times 3 \times 3$, $4 \times 4 \times 3$, $5 \times 5 \times 3$, $6 \times 6 \times 3$, $7 \times 7 \times 3$ and $8 \times 8 \times 3$ CNTs represent the pure CNTs of the $C_{36}H_{12}$, $C_{48}H_{16}$, $C_{60}H_{20}$, $C_{72}H_{24}$, $C_{84}H_{28}$ and $C_{96}H_{32}$ CNTs with various diameters, respectively. To make the boron (B), aluminum (Al), gallium (Ga), silicon (Si), germanium (Ge), nitrogen (Ni), phosphorus (P), and arsenic (As) doped CNTs, one C atom of each model has been substituted by one B, Al, Ga, Si, Ge, N, P and As atom. In order to model the doped CNTs, a dopant atom from the central region of the nanotubes (X position in Fig. 1) was substituted with a carbon atom before optimization starts. Both ends of the pure and doped CNTs were capped with hydrogen atoms to saturate dangling bonds

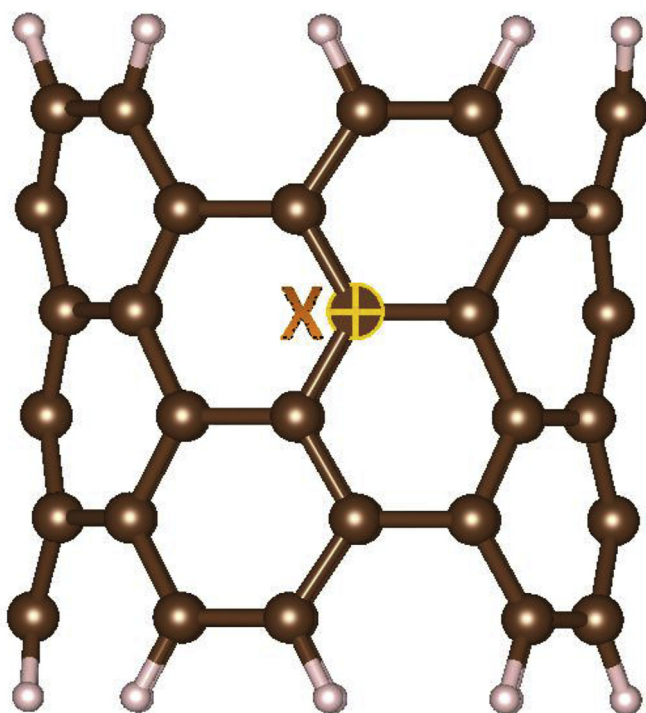


Fig. 1. (Colour online) A schematic side view of $6 \times 6 \times 3$ CNT. X position on which the doped atom is placed at the beginning of optimization.

due to fragment stabilization effect in the system [32]. The pure and doped CNTs were fully optimized without any symmetry constraints at the B3LYP/6-31G(d) level [33] by Gaussian 09 [34]. We have carried out these basis set and method due to our limited computational resources and time constraints. Moreover, the previous first-principles calculations show that the B3LYP method works on pure and doped CNTs [35–37] very well.

VIP and VEA of optimized pure and doped CNTs are calculated by the following formulas,

$$VIP = E^+ - E^0 \quad (1)$$

$$VEA = E^0 - E^- \quad (2)$$

where E^0 , E^+ and E^- are the neutral, cation and anion energies of pure and doped CNTs, respectively. VIP is defined as the difference between the energy of cation at optimized neutral geometry and the energy of optimized neutral. VEA is defined as the difference between the energy of optimized neutral and the energy of cation at optimized neutral geometry. Using the VIP and VEA energies, the chemical hardness (η), chemical softness (σ), chemical potential (μ), electronegativity (χ), electrophilicity (ω), maximum amount of electronic charge index (ΔN_{tot}), electron accepting (ω^+) and donating capability (ω^-) can be calculated [38–40] as following: $\eta = (VIP - VEA)/2$, $\sigma = 1/2\eta$, $\mu = -(VIP + VEA)/2$, $\chi = (VIP + VEA)/2$, $\omega = \mu^2/2\eta$, $\Delta N_{tot} = -\mu/\eta$, $\omega^+ = (3 \times VIP + VEA)/[16 \times (VIP - VEA)]$, $\omega^- = (VIP + 3 \times VEA)/[16 \times (VIP - VEA)]$. Total density of states (DOS) of the CNTs is carried out by the GaussSum 3.0 program [41]. At the optimized structures of the CNTs, there are no imaginary (negative) frequency modes, indicating that the optimized structures are on the real minimum potential energy surface was found.

3. Results and discussions

3.1. Structure, energy and stability

In this study, we performed a comprehensive study on III-, IV-, and V. group elements doped CNTs with different diameters. Fig. 1 indicate, as an example, that the initial geometry of a single atom doped CNT obtained by replacing the middle carbon atom in CNTs by B, Al, Ga, Si, Ge, N, P and As atoms. A schematic side and top views of optimized pure CNTs in different diameters are shown in Fig. 2. Studied pure CNTs have diameters in the range of 4–11 Å (see Fig. 2), which is compatible with the usual CNTs observed in experiments [42,43]. In addition, all the geometries of optimized structures for the pure and doped CNTs are presented as supporting information (see Figs. S1–S6). After fully structural optimizations, there is no considerable structural distortion in the B- and N-doped CNTs (see Figs. S1–S6). Because B and N atoms have approximately the same atomic radius with C atom. Al-, Si-, P-, Ga-, Ge- and As-doped CNTs are slightly destroyed the cylinder form of considered CNTs (see Figs. S1–S6). The positions of the nearest C atoms of doped atoms except for B and N are out of the CNT surface with different degrees.

The total energies (E_{tot}), binding energy per atom (E_b) and formation energy (E_f) of the optimized pure and doped CNTs are presented in Table S1 (see Supporting Information). Using the total energy calculations, E_b and E_f can be given,

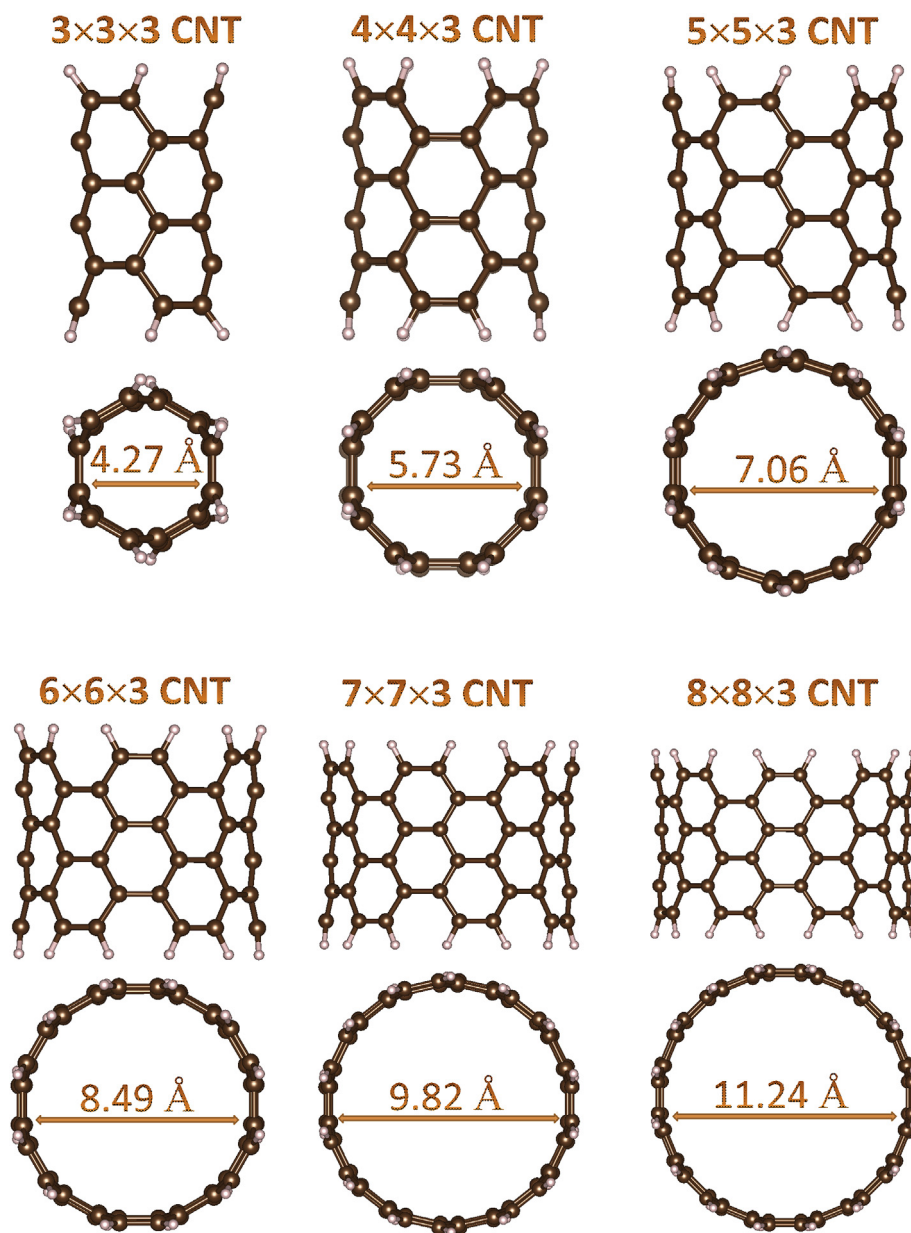


Fig. 2. (Colour online) Side and top views of optimized pure CNTs in different diameters.

$$E_b = [i \times E(C) + j \times E(H) + E(\text{doped atom}) - E(\text{doped CNT})] \times / (i + j + 1) \quad (3)$$

$$E_f = E(\text{doped CNT}) - E(\text{CNT}) - E(\text{doped atom}) + E(C) \quad (4)$$

where $E(C)$, $E(H)$ and $E(\text{doped atom})$ are E_{tot} of one C, one H and doped atom, respectively. $E(\text{doped-CNT})$ is E_{tot} of the atom doped-CNT, and $E(\text{CNT})$ is E_{tot} for pure CNT. i and j in equation (1) are also the number of C and H atoms for pure or doped CNTs, respectively.

Fig. 3 shows that the results for the E_b of pure and doped CNTs. When one B, Al, Ga, Si, Ge, N, P and As atom is doped to pure CNTs, E_b is decreased (see Fig. 3). E_b values of doped CNTs are found to be in the following decreasing order: CNT-N > CNT-B > CNT-P > CNT-

Si > CNT-As > CNT-Ge > CNT-Al > CNT-Ga. Compared with the doped CNTs, the stabilities of N- and B-doped CNTs are higher than that of the others. It is well known that electronegativity is a measure of the ability of an atom to attract the electrons. Electronegativity generally increases from left to right across in periodic table while it generally decreases from top to bottom of a group. Meanwhile, N atom has the highest electronegativity while Ga atom has the lowest electronegativity. This may be the reason that N-doped CNTs have higher E_b than Ga-doped CNTs. In the literature, the effects of substitutional dopants on the C_{20} were studied [44,45]. For example, the stability of $C_{12}X_8$ heterofullerenes where X = B, Al, Ga, C, Si, Ge, N, P, and As was investigated and found C=C bond lengths decrease slightly as going from $C_{12}N_8$ and $C_{12}B_8$ to $C_{12}Ga_8$ and $C_{12}Al_8$ [45]. In the study, the results showed that the E_b of $C_{12}Ga_8$ and $C_{12}Al_8$ are less than those of $C_{12}B_8$ and $C_{12}N_8$. Moreover, it is reported in these studies that the stability of N-doped CNTs is higher than the Ga-doped CNTs because the C=C

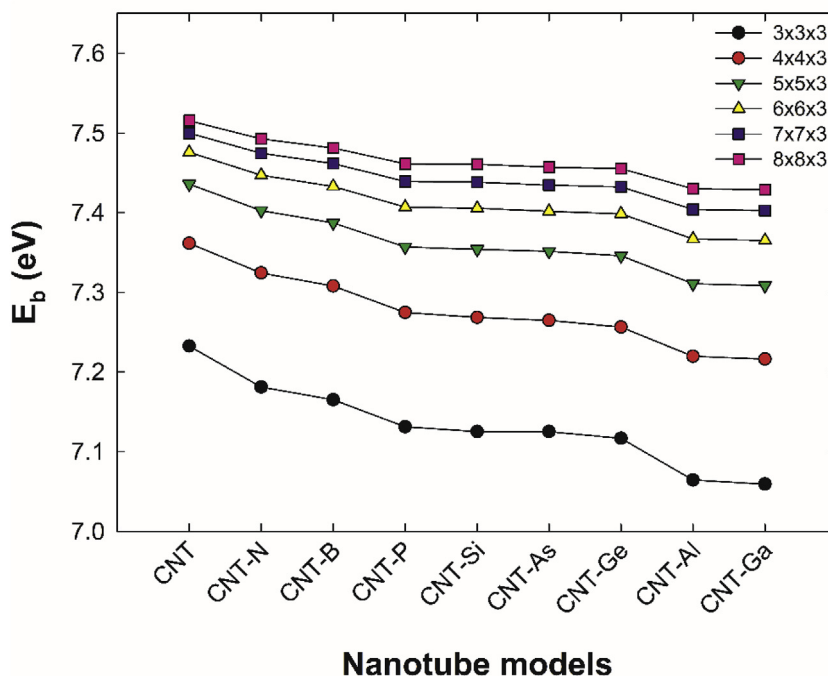


Fig. 3. (Colour online) Binding energy per atom (E_b) for substituted CNTs obtained at B3LYP/6-31G(d) level of theory.

bond lengths of *N*-doped CNTs are shorter than that of Ga-doped CNTs. Therefore, all the mentioned above examples can be explained why different dopant gives different results. In addition, the stabilities of *N*- and B-doped CNTs are in agreement with previous studies [46–48]. On the other hand, Ga-doped CNTs have been found to be effective for drug adsorption [49]. According to E_b , B and *N*-doped CNTs would be more effective for drug adsorption than Ga-doped CNTs due to its high value. On the other hand, E_b of pure and doped CNTs increases with an increase in diameter from 4.27 to 11.24 Å. In addition, the E_b of pure CNTs are found to be in the following increasing order: $3 \times 3 \times 3 < 4 \times 4 \times 3 < 5 \times 5 \times 3 < 6 \times 6 \times 3 < 7 \times 7 \times 3 < 8 \times 8 \times 3$ (see Fig. 3). These results indicate that stability increases depending on an increase in diameter of CNTs. The previous studies have shown that the CNTs with larger diameter has higher thermal stability than smaller-diameter CNTs [50–52].

Fig. 4 shows that the results for the E_f of doped CNTs. From Fig. 4, E_f is significantly decreased when one B, Al, Ga, Si, Ge, N, P and As atom is doped to pure CNTs. E_f drops to the range of 2–3 eV, which is E_f for *N*-doped CNTs. This indicates that the *N*-doped CNTs needs a smaller energy cost to substitute a carbon atom with an N atom. It is very compatible with our previous results [53]. However, Ga-doped CNTs need much greater energy (in range of 8–11 eV) cost than that of the other CNTs. Note that the *N*-doped CNTs become more preferable in energy than other doped-CNTs. Compared with the doped CNTs, the $3 \times 3 \times 3$ doped CNTs need less energy than other doped CNTs and thus they become more preferable in energy than others. We should also mention that pure and doped CNTs have similar trends in energetic analyses such as E_b and E_f .

3.2. Electronic and optical properties

The vertical ionization potential (VIP), vertical electron affinity (VEA), density of state (DOS) and the energy gap (E_g) between the highest occupied molecular orbital (HOMO) and the lowest unoccupied molecular orbital (LUMO) of the optimized the pure and

doped CNTs are tabulated in Table S1.

Fig. 5 shows that the results for the E_g of pure and doped CNTs. When B, Al, Ga, Si, Ge, N, P and As atoms are doped to pure CNTs, E_g shows a decreasing trend. It drops to a value below 1 eV for B-doped and *N*-doped $n \times n \times 3$ ($n = 4–8$) CNTs. According to our preferred sort order, E_g of the *N*-doped $3 \times 3 \times 3$ CNT and As-doped $4 \times 4 \times 3$ CNT gives a pick. Except those and some pure $4 \times 4 \times 3$ CNTs, E_g values of all CNTs are generally found to be in the following decreasing order: CNT > CNT-Si > CNT-Ge > CNT-P > CNT-As > CNT-Al > CNT-Ga > CNT-N > CNT-B. E_g of the pure and doped $3 \times 3 \times 3$ CNTs is higher than that of other CNTs. In addition, the E_g of Si-, Ge-, P- and As-doped CNTs importantly decreases with an increase in the diameter of CNTs (excluding $3 \times 3 \times 3$ CNTs), whereas those of Al-, Ga-, *N*- and B-doped CNTs slightly reduces with an decrease in the diameter of CNTs. E_g values of pure CNTs are also found to be in the following increasing order: $4 \times 4 \times 3$ CNT < $5 \times 5 \times 3$ CNT < $6 \times 6 \times 3$ CNT < $7 \times 7 \times 3$ CNT < $8 \times 8 \times 3$ CNT < $3 \times 3 \times 3$ CNT.

We note that the electrical conductivity of the all-pure CNTs changes considerably with doping of one atom. However, $3 \times 3 \times 3$ CNTs are weaker in electronic conductivity than other CNTs due to having the highest band gap. It is important that B-doped and *N*-doped CNTs with the lowering of the band gaps can be preferred for optoelectronic applications because the electronic transfer is easier. This also indicates that B-doped and *N*-doped CNTs compared to that of the pure and other doped CNTs allows easy excitation of electrons from HOMO to LUMO. It is interesting to note that after B- and *N*-doping, the E_g of CNTs changes drastically. CNTs can act as a semiconductor or conductor, depending on its diameters [54,55]. The previous studies have shown that the type of CNT changes from semiconductor to conductor after *N*-doping [56,57]. Moreover, it is reported that the replacing the B/N in pure CNTs causes to the formation of a new band in the band structure and the B/N doped CNT becomes as p-/n-type semiconductor [48].

Fig. 6 shows that the results for the DOS of pure and doped CNTs. The DOS provides general information on the electronic structure and the band energy of the CNTs. In this study, the DOS was

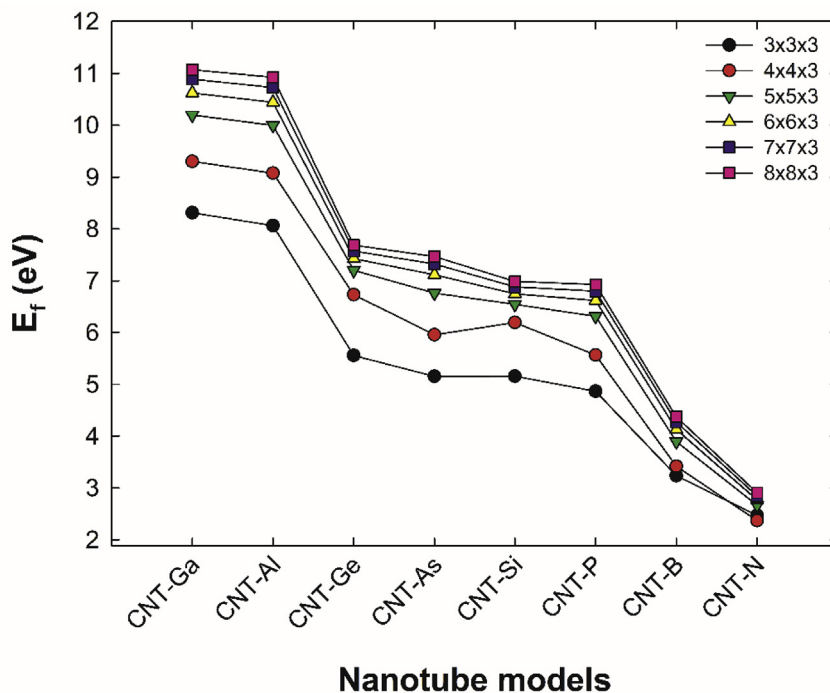


Fig. 4. (Colour online) Formation energy (E_f) for substituted CNTs obtained at B3LYP/6-31G(d) level of theory.

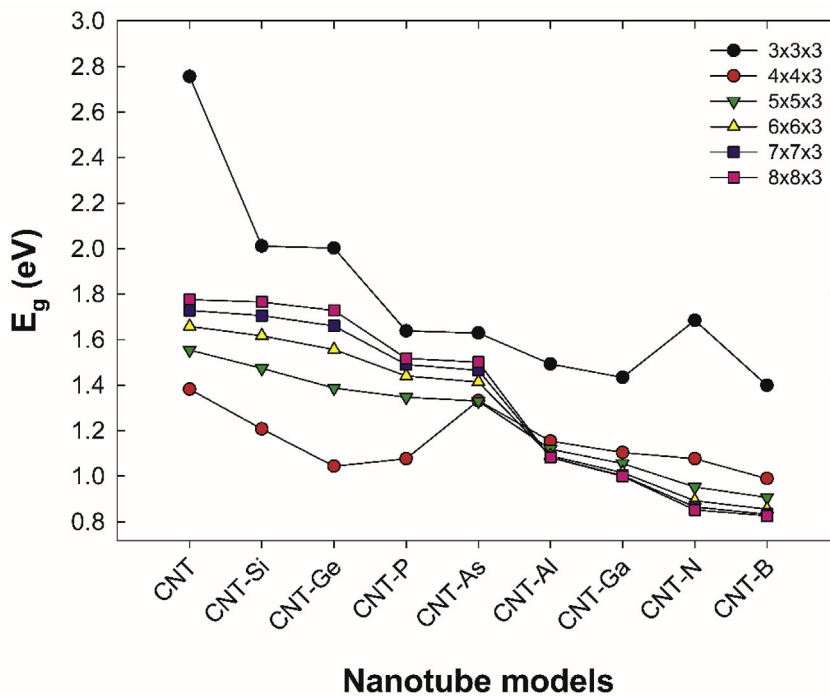


Fig. 5. (Colour online) HOMO-LUMO energy gap (E_g) for substituted CNTs obtained at B3LYP/6-31G(d) level of theory.

calculated in the energy range -7 to 0 eV. The DOS plots of the CNTs show a sign anomaly change in the gap regions. In addition, the band gap energy of CNTs is significantly decreased when B, Al, Ga, Si, Ge, N, P and As atoms are doped to pure CNTs and thus electrical conductance increases. Note that a high DOS corresponds to available states for occupation at each energy level.

Fig. 7 shows that the results for the VIP of pure and doped CNTs.

The values of VIP remain constant around 5.2 eV when B, Al, Ga, Si, Ge, P and As atoms are doped to pure $4 \times 4 \times 3$, $5 \times 5 \times 3$, $6 \times 6 \times 3$, $7 \times 7 \times 3$, $8 \times 8 \times 3$ CNTs, whereas N-doped CNTs of those are significantly decreased. Similarly, the values of VIP remain approximately constant at 6 eV when Si and Ge atoms are doped to pure $3 \times 3 \times 3$ CNTs. VIP value of N-doped $3 \times 3 \times 3$ CNT is also lower than those of other doped $3 \times 3 \times 3$ CNTs. In addition, VIP

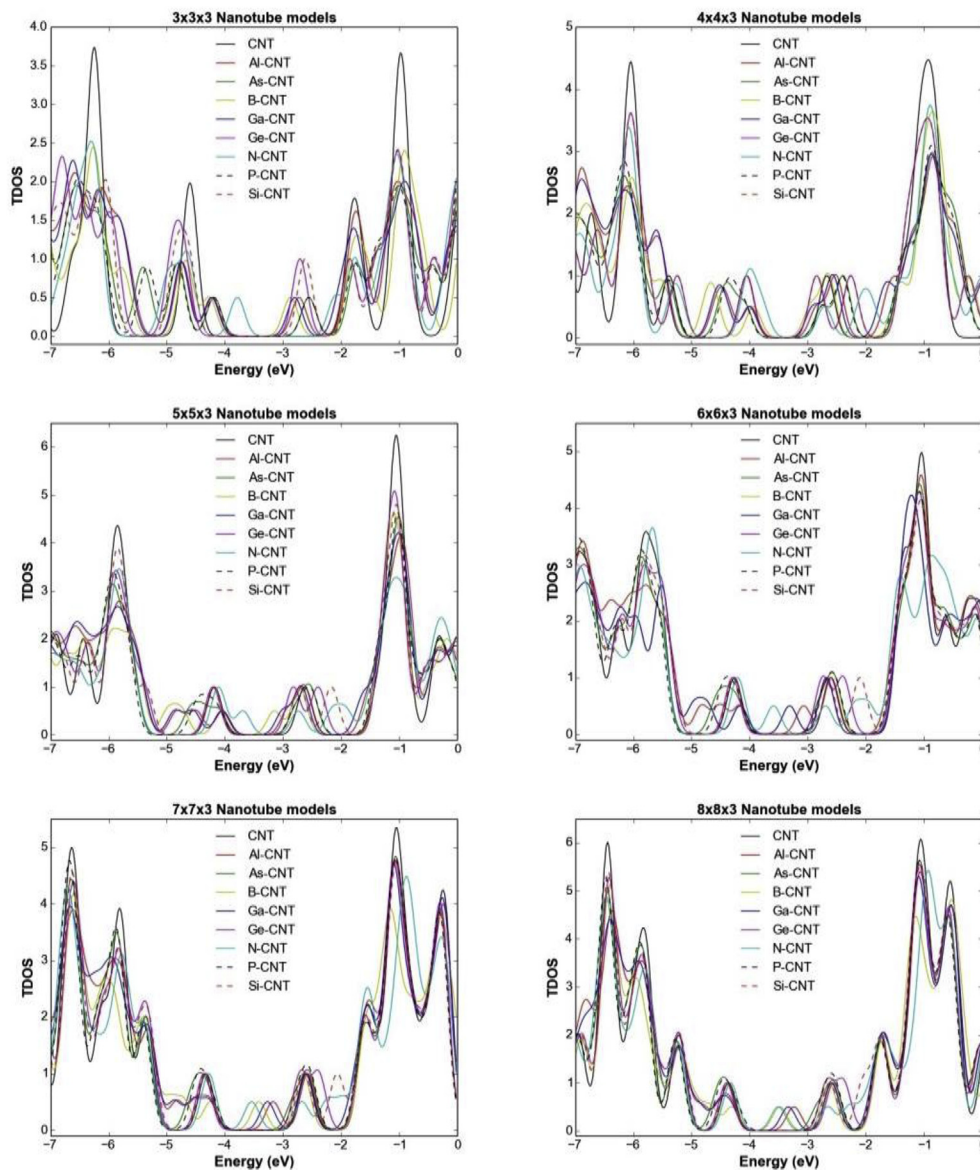


Fig. 6. (Colour online) Total densities of states (TDOS) for substituted CNTs obtained at B3LYP/6-31G(d) level of theory.

values of pure and doped $3 \times 3 \times 3$ CNTs are higher than those of other pure and doped CNTs and thus a removal electron is more difficult for $3 \times 3 \times 3$ CNTs. This also indicates that the pure and doped $3 \times 3 \times 3$ CNTs are higher stability than others.

Fig. 8 shows the results for the VEA of pure and doped CNTs. VEA shows an increasing trend as B, Al, Ga, Si, Ge, N, P and As atoms are doped to pure CNTs. VEA of the Ge-doped and Si-doped $3 \times 3 \times 3$ and $4 \times 4 \times 3$ CNTs gives a pick, whereas VEA values of B-doped CNTs are generally higher than those of other doped CNTs. Except for doped $3 \times 3 \times 3$ and $4 \times 4 \times 3$ CNTs, VEA values of all CNTs are generally found to be in the following increasing order: CNT < CNT-Si < CNT-N < CNT-Ge < CNT-P < CNT-As < CNT-Al < CNT-Ga < CNT-B. In addition, VEA of all CNTs is generally found to be in the following increasing order: $3 \times 3 \times 3$ CNT < $4 \times 4 \times 3$ CNT < $5 \times 5 \times 3$ CNT < $6 \times 6 \times 3$ CNT < $7 \times 7 \times 3$ CNT < $8 \times 8 \times 3$ CNT. We should also mention that the electron affinity of $3 \times 3 \times 3$ and $4 \times 4 \times 3$ Ge-doped and Si-doped CNTs is significantly increased because they can be preferred to use in optoelectronic applications. It is very compatible with our previous results [53]. Especially, B-

doped CNTs with the rising of the VEA can be preferred for optoelectronic applications or devices, which prefer higher electron affinity, because the electronic transfer is easier.

3.3. Global reactivity

The reactivity properties of pure and doped CNTs are discussed in terms of the η , chemical softness (σ), chemical potential (μ), electronegativity (χ), electrophilicity (ω), maximum amount of electronic charge index (ΔN_{tot}), electron accepting (ω^+) and donating (ω^-) capability calculated at B3LYP/6-31G(d) level of theory. These parameters are presented in Table S2 (see Supporting Information). Fig. 9 shows that the results for the η of pure and doped CNTs. η shows a decrease trend when B, Al, Ga, Si, Ge, N, P and As atoms are doped to pure CNTs. Except doped $3 \times 3 \times 3$ and $4 \times 4 \times 3$ CNTs, η values of all CNTs are found to be in the following decreasing order: CNT > CNT-Si > CNT-Ge > CNT-P > CNT-As > CNT-Al > CNT-Ga > CNT-Na > CNT-B. In addition, η values of $3 \times 3 \times 3$ CNTs are higher than those of other CNTs, thus indicating a higher

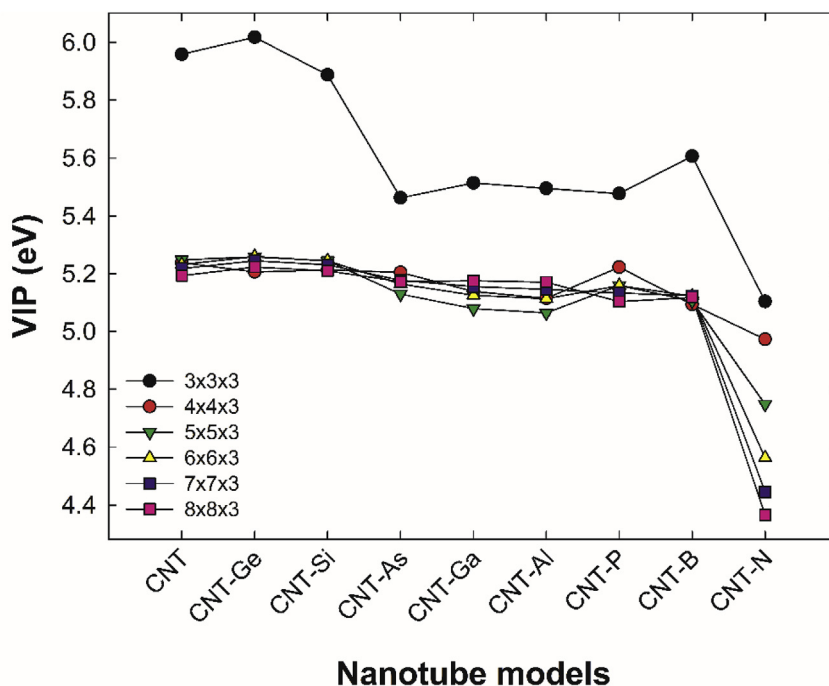


Fig. 7. (Colour online) Vertical ionization potential (VIP) for substituted CNTs obtained at B3LYP/6-31G(d) level of theory.

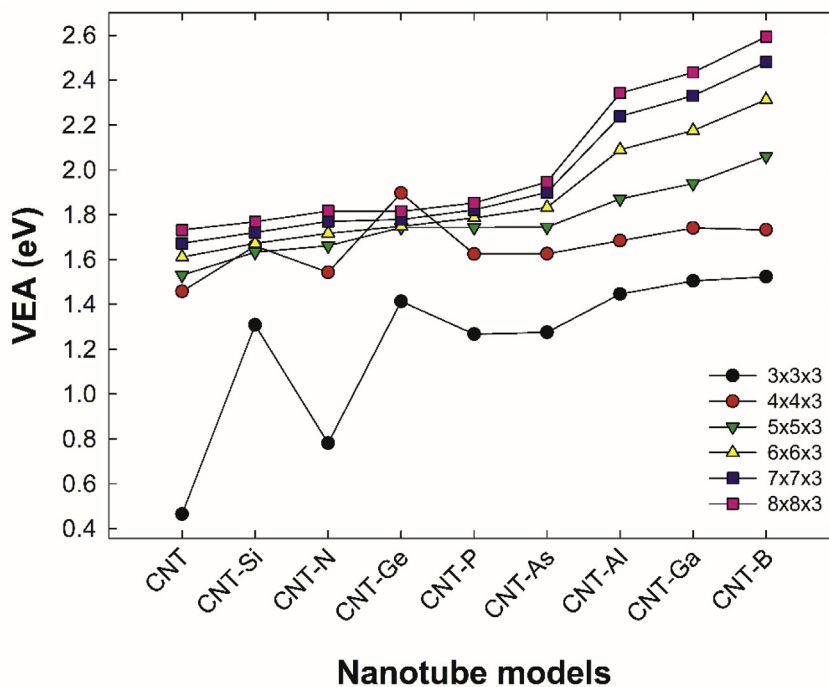


Fig. 8. (Colour online) Vertical electron affinity (VEA) for substituted CNTs obtained at B3LYP/6-31G(d) level of theory.

resistance to charge transfer and change in the band structure. A more hard structure leads to a larger ionization potential and a smaller electron affinity as well as a more large energy gap [58], which implies that a lower tendency to give an electron and the structure is more stable. In this study, η significantly decreases for B-, N- and Ga- doped CNTs. Thus, B-, N- and Ga-doped CNTs have more reactivity than pure and other doped CNTs. The previous studies show that η decreases by doping of Ga in CNTs [49].

Therefore, our results agree with the literature.

Fig. 10 shows that the results for the ω of pure and doped CNTs. ω shows an increase trend as B, Al, Ga, Si, Ge, N, P and As atoms are doped to pure CNTs. ω values of $3 \times 3 \times 3$ CNTs are lower than those of other CNTs. Moreover, ω values of CNTs are generally found to be in the following increasing order: CNT < CNT-Si < CNT-N < CNT-Ge < CNT-P < CNT-As < CNT-Al < CNT-Ga < CNT-B. However, ω of the Si-doped and Ge-doped $3 \times 3 \times 3$ and $4 \times 4 \times 3$ CNTs gives a

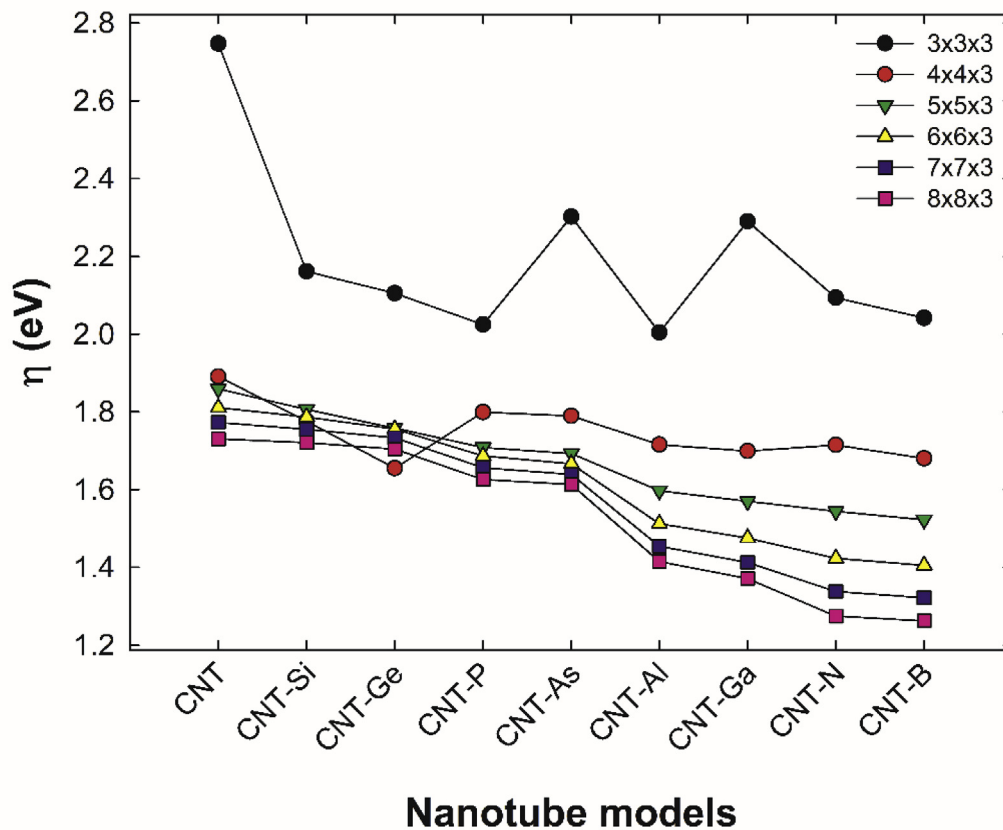


Fig. 9. (Colour online) Chemical hardness (η) for substituted CNTs obtained at B3LYP/6-31G(d) level of theory.

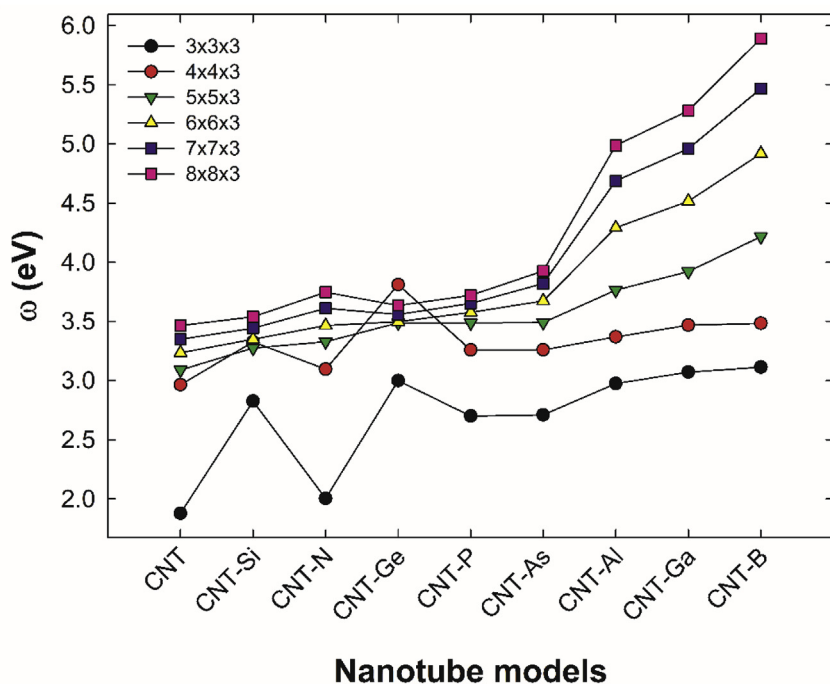


Fig. 10. (Colour online) Electrophilicity index (ω) for substituted CNTs obtained at B3LYP/6-31G(d) level of theory.

pick similar to the VEA graph, which prefers higher electron affinity. Except those, ω of CNTs are generally found to be in the following increasing order: $3 \times 3 \times 3$ CNT $< 4 \times 4 \times 3$ CNT $< 5 \times 5 \times 3$ CNT $< 6 \times 6 \times 3$ CNT $< 7 \times 7 \times 3$ CNT $< 8 \times 8 \times 3$ CNT. In addition, the ω^- and ω^+ values are increased as B, Al, Ga, Si, Ge, N, P and As atoms are doped to pure CNTs (see Table S2, at Supporting Information). Note that the electron affinities of the doped CNTs are also much further from the pure CNTs. Especially, the electrophilicity and electron affinity of the B- and Ga-doped CNTs are higher than those of other doped CNTs. The ω , ω^- , and ω^+ are a measure of electrophilic power of the system. The stability of the B, Al, Ga, Si, Ge, N, P and As-doped CNTs decrease and their reactivity increase which is in agreement with previous studies [49].

Fig. 11 shows that the results for the ΔN_{tot} of pure and doped CNTs. When B, Al, Ga, Si, Ge, N, P and As atoms are doped to pure CNTs, ΔN_{tot} shows an increasing trend. ΔN_{tot} values of $3 \times 3 \times 3$ CNTs are lower than those of other CNTs. The ΔN_{tot} of the N-doped $3 \times 3 \times 3$ CNT gives a dip and it has the lowest value in the doped $3 \times 3 \times 3$ CNTs, whereas, those of Ge-doped $4 \times 4 \times 3$ CNT gives a pick and it has the highest value in the all $4 \times 4 \times 3$ CNTs. Except for $3 \times 3 \times 3$ and $4 \times 4 \times 3$ CNTs, ΔN_{tot} values are generally found to be in the following increasing order: CNT $<$ CNT-Si $<$ CNT-Ge $<$ CNT-P $<$ CNT-As $<$ CNT-N $<$ CNT-Al $<$ CNT-Ga $<$ CNT-B. In addition, except Ge-doped $4 \times 4 \times 3$ CNT, ΔN_{tot} values are found to be in the following increasing order: $3 \times 3 \times 3$ CNT $<$ $4 \times 4 \times 3$ CNT $<$ $5 \times 5 \times 3$ CNT $<$ $6 \times 6 \times 3$ CNT $<$ $7 \times 7 \times 3$ CNT $<$ $8 \times 8 \times 3$ CNT. When one B atom is doped to CNTs, the accepting electron has become more effective than others. This result implies that the B-doped CNTs have the most accepted electron charge. We should also mention that all CNTs except $3 \times 3 \times 3$ and $4 \times 4 \times 3$ have generally similar trends in electronic properties such as VIP, VEA, η , ω ΔN_{tot} . There is a decrease in the η , E_g , and VIP is due to B, Al, Ga, Si, Ge, N, P and As atoms doping processes. As a result, the stability of the considered CNTs is lower and thus their reactivity increases.

3.4. Non-linear optical properties

The non-linear optical (NLO) properties are discussed in terms of dipole moment (μ), mean static polarizability (α_{tot}), anisotropic polarizability ($\Delta\alpha$) and first-order hyperpolarizability (β). NLO properties in terms of x, y, z tensor components can be carried out

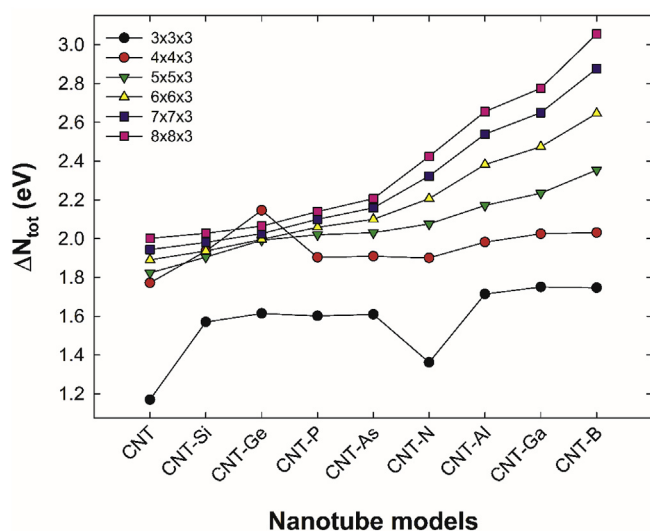


Fig. 11. (Colour online) Maximum amount of electronic charge index (ΔN_{max}) for substituted CNTs obtained at B3LYP/6-31G(d) level of theory.

based on the same methodology as reported [59,60]. NLO properties of the pure and doped CNTs at B3LYP/6-31G(d) level of theory are summarized in Table S3 (see Supporting Information).

From Table S3, it can be found that the mean static polarizability (α_{tot}) and anisotropic polarizability ($\Delta\alpha$) values increase prominently as B, Al, Ga, Si, Ge, N, P and As atoms are doped to pure CNTs. Urea is the first molecule calculated NLO properties, and thus it is used as a reference for comparison [61–63]. All the pure CNTs showed a lower value for β in comparison with urea (0.371×10^{-30} esu). From Table S3, however, it can be found that β is available to enhance when B, Al, Ga, Si, Ge, N, P and As atoms are doped to pure CNTs. In addition, all the doped CNTs show enhanced the β values in comparison with urea. From Table S3, Al- and Ga-doping are a more effective way to improve significantly the nonlinear optical properties of all the CNTs. Similarly, B- and N-doping are also an effective way to importantly increase the NLO properties of $5 \times 5 \times 3$, $6 \times 6 \times 3$, $7 \times 7 \times 3$ and $8 \times 8 \times 3$ CNTs. It is reported that a structure to be considered a viable candidate should have β greater than approximately 500×10^{-30} esu [64]. Therefore, our results indicate that B-, Al-, Ga- and N-doped $8 \times 8 \times 3$ CNTs should also have considered being a viable candidate for further studies. We should also mention that all the doped CNTs exhibit a good NLO activity.

3.5. The refractive index (n)

The refractive index (n) values of the CNTs were calculated from Ravindra relation [65], which is defined as:

$$n = 4.084 - 0.62E_g \quad (5)$$

where E_g is HOMO-LUMO gap which represents a linear relation. Based on the doped atom and diameter, the CNTs have different n values (see Fig. 12). For example, the n of the pure $3 \times 3 \times 3$ CNT is 2.37 (the smallest), while the $4 \times 4 \times 3$ is 3.22 (the greatest). When it comes to the atom doped CNTs, B-doped CNTs $7 \times 7 \times 3$ and $8 \times 8 \times 3$ are found to be 3.56 (the biggest value), however, Si- and Ge-doped CNTs is almost 2.84 (the smallest value). From the results obtained, one can conclude that the value of n for CNTs can be controlled with changing the diameter of CNTs and substituted different atoms on CNTs.

4. Conclusions

We have studied the structural, electronic, reactivity, non-linear optical and optoelectronic properties of the pure and B-, Al-, As-, Si-, Ge-, N-, P-, and As-doped CNTs with different diameters by DFT at B3LYP/6-31G(d) level. The analyses of the energetic show that the binding energy, formation energy, and chemical hardness are decreased when B, Al, Ga, Si, Ge, N, P and As atoms are doped to CNTs. These results indicate that the stabilities decrease depending on doping additives of pure CNTs. However, the stability of CNTs increases with an increase in the diameter of CNTs. More importantly, the band gap is decreased as B, Al, Ga, Si, Ge, N, P and As atoms are doped to CNTs. Our results show that B-doping decreases greatly band gap from 2.76 eV to 0.83 eV. Therefore, it appears to be the most effective for electronic conductivity. We found that the E_g of Si-, Ge-, P- and As-doped CNTs significantly decreases with an increase in the diameter of the CNTs (except $3 \times 3 \times 3$ CNTs). However, the band gaps of Al-, Ga-, N- and B-doped CNTs slightly reduce with a decrease in the diameter of CNTs. It is interesting to note that the band gaps are changed as directly or inversely proportional with diameter depending on the type of doping atoms. Therefore, it is of great interest to produce CNTs with the desired diameter. The analyses of the reactivity show that electrophilicity

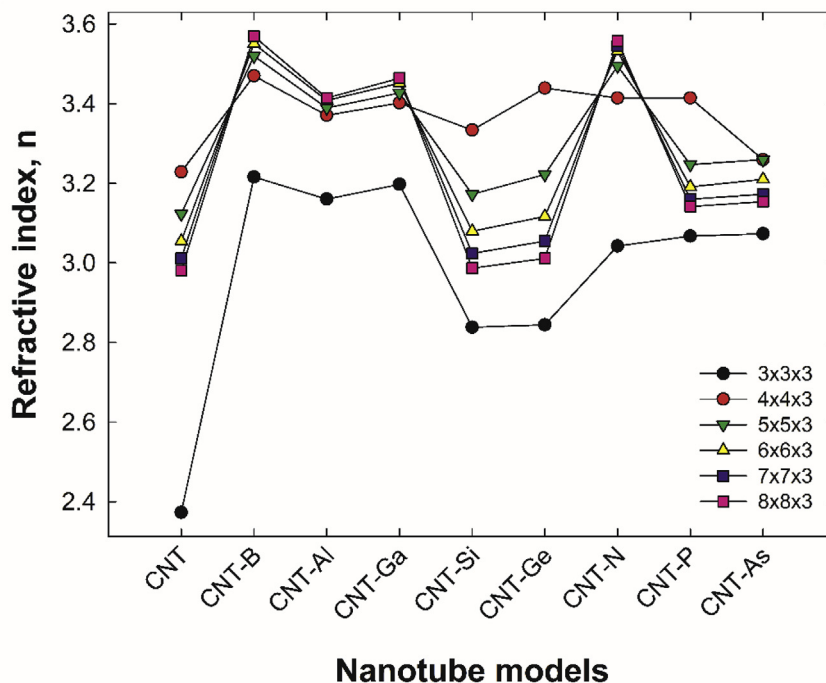


Fig. 12. (Colour online) Refractive index (n) for substituted CNTs obtained at B3LYP/6-31G(d) level of theory.

and maximum amount of electronic charge indexes are increased as B, Al, Ga, Si, Ge, N, P and As atoms are doped to CNTs. In addition, B-doping appears to be the most effective for accepting an electron. Note that all the doped CNTs exhibit a good NLO activity. Especially, B-, Al-, Ga- and N- doping are an effective way to enhance the nonlinear optical properties of the CNTs. We believe that this study will be useful for better understanding the nature of the CNTs as well as a powerful tool for experimental researches in the future.

Supporting Information

Supporting information includes the graphical pictures of all optimized structures for pure and doped CNTs obtained at B3LYP/6-31G(d) level of theory, as well as the structural, electronic, reactivity and non-linear optical (NLO) properties of pure and doped all-CNTs.

Appendix A. Supplementary data

Supplementary data to this article can be found online at <https://doi.org/10.1016/j.jallcom.2019.06.210>.

References

- [1] P. Li, W. Chen, Recent advances in one-dimensional nanostructures for energy electrocatalysis, *Chin. J. Catal.* 40 (2019) 4–22. [https://doi.org/10.1016/S1872-2067\(18\)63177-8](https://doi.org/10.1016/S1872-2067(18)63177-8).
- [2] Q. Xu, W. Li, L. Ding, W. Yang, H. Xiao, W.-J. Ong, Function-driven engineering of 1D carbon nanotubes and 0D carbon dots: mechanism, properties and applications, *Nanoscale* 11 (2019) 1475–1504. <https://doi.org/10.1039/c8nr08738e>.
- [3] L. Mai, J. Sheng, L. Xu, S. Tan, J. Meng, One-dimensional hetero-nanostructures for rechargeable batteries, *Acc. Chem. Res.* 51 (2018) 950–959. <https://doi.org/10.1021/acs.accounts.8b00031>.
- [4] M. Kurban, Ş. Erkoç, Mechanical properties of CdZnTe nanowires under uniaxial stretching and compression: a molecular dynamics simulation study, *Comput. Mater. Sci.* 122 (2016) 295–300. <https://doi.org/10.1016/j.commatsci.2016.05.041>.
- [5] P. Zhao, P. Wang, Z. Zhang, C. Fang, Y. Wang, Y. Zhai, D. Liu, Electronic transport properties of a diarylethene-based molecular switch with single-

- walled carbon nanotube electrodes: the effect of chirality, *Solid State Commun.* 149 (2009) 928–931. <https://doi.org/10.1016/j.ssc.2009.03.027>.
- [6] P. Zhao, P.J. Wang, Z. Zhang, D.S. Liu, Negative differential resistance in a carbon nanotube-based molecular junction, *Phys. Lett.* 374 (2010) 1167–1171. <https://doi.org/10.1016/j.physleta.2009.12.047>.
- [7] S.H. Ng, J. Wang, Z.P. Guo, J. Chen, G.X. Wang, H.K. Liu, Single wall carbon nanotube paper as anode for lithium-ion battery, *Electrochim. Acta* 51 (2005) 23–28. <https://doi.org/10.1016/j.electacta.2005.04.045>.
- [8] G. Vijayaraghavan, K.J. Stevenson, Synergistic assembly of dendrimer-templated platinum catalysts on nitrogen-doped carbon nanotube electrodes for oxygen reduction, *Langmuir* 23 (2007) 5279–5282. <https://doi.org/10.1021/la0637263>.
- [9] L. Lindsay, D.A. Broido, N. Mingo, Diameter dependence of carbon nanotube thermal conductivity and extension to the graphene limit, *Phys. Rev. B* 82 (2010). <https://doi.org/10.1103/PhysRevB.82.161402>.
- [10] E. Pop, D. Mann, Q. Wang, K.E. Goodson, H.J. Dai, Thermal conductance of an individual single-wall carbon nanotube above room temperature, *Nano Lett.* 6 (2006) 96–100. <https://doi.org/10.1021/nl052145f>.
- [11] M. Fujii, X. Zhang, H.Q. Xie, H. Ago, K. Takahashi, T. Ikuta, H. Abe, T. Shimizu, Measuring the thermal conductivity of a single carbon nanotube, *Phys. Rev. Lett.* 95 (2005). <https://doi.org/10.1103/PhysRevLett.95.065502>.
- [12] Z. Chen, D. Higgins, Z. Chen, Nitrogen doped carbon nanotubes and their impact on the oxygen reduction reaction in fuel cells, *Carbon N. Y.* 48 (2010) 3057–3065. <https://doi.org/10.1016/j.carbon.2010.04.038>.
- [13] L. Yang, S. Jiang, Y. Zhao, L. Zhu, S. Chen, X. Wang, Q. Wu, J. Ma, Y. Ma, Z. Hu, Boron-doped carbon nanotubes as metal-free electrocatalysts for the oxygen reduction reaction, *Angew. Chem. Int. Ed.* 50 (2011) 7132–7135. <https://doi.org/10.1002/anie.201101287>.
- [14] E. Poirier, R. Chahine, P. Benard, D. Cossement, L. Lafi, E. Melancon, T.K. Bose, S. Desilets, Storage of hydrogen on single-walled carbon nanotubes and other carbon structures, *Appl. Phys. Mater. Sci. Process* 78 (2004) 961–967. <https://doi.org/10.1007/s00339-003-2415-y>.
- [15] J. Ye, Q. Shao, X. Wang, T. Wang, Effects of B, N, P and B/N, B/P pair into zigzag single-walled carbon nanotubes: a first-principle study, *Chem. Phys. Lett.* 646 (2016) 95–101. <https://doi.org/10.1016/j.cpllett.2015.12.056>.
- [16] A. Hansson, M. Paulsson, S. Stafstrom, Effect of bending and vacancies on the conductance of carbon nanotubes, *Phys. Rev. B* 62 (2000) 7639–7644. <https://doi.org/10.1103/PhysRevB.62.7639>.
- [17] S.B. Fagan, R. Mota, A.J.R. da Silva, A. Fazzio, Ab initio study of an iron atom interacting with single-wall carbon nanotubes, *Phys. Rev. B* 67 (2003). <https://doi.org/10.1103/PhysRevB.67.205414>.
- [18] T. Koretsune, S. Saito, Electronic structure of boron-doped carbon nanotubes, *Phys. Rev. B* 77 (2008). <https://doi.org/10.1103/PhysRevB.77.165417>.
- [19] W.-H. Chiang, G.-L. Chen, C.-Y. Hsieh, S.-C. Lo, Controllable boron doping of carbon nanotubes with tunable dopant functionalities: an effective strategy toward carbon materials with enhanced electrical properties, *RSC Adv.* 5 (2015) 97579–97588. <https://doi.org/10.1039/c5ra20664b>.

- [20] J. Lu, X. Zhang, X. Wu, Z. Dai, J. Zhang, A Ni-doped carbon nanotube sensor for detecting oil-dissolved gases in transformers, *Sensors* 15 (2015) 13522–13532, <https://doi.org/10.3390/s150613522>.
- [21] B. Shan, K. Cho, Oxygen dissociation on nitrogen-doped single wall nanotube: a first-principles study, *Chem. Phys. Lett.* 492 (2010) 131–136, <https://doi.org/10.1016/j.cplett.2010.04.050>.
- [22] K. Gong, F. Du, Z. Xia, M. Durstok, L. Dai, Nitrogen-doped carbon nanotube Arrays with high electrocatalytic activity for oxygen reduction, *Science* 323 (2009) 760–764, <https://doi.org/10.1126/science.1168049>, 80-.
- [23] L. Qu, Y. Liu, J.-B. Baek, L. Dai, Nitrogen-doped graphene as efficient metal-free electrocatalyst for oxygen reduction in fuel cells, *ACS Nano* 4 (2010) 1321–1326, <https://doi.org/10.1021/nn901850u>.
- [24] Z. Zhang, K. Cho, Ab initio study of hydrogen interaction with pure and nitrogen-doped carbon nanotubes, *Phys. Rev. B* 75 (2007), <https://doi.org/10.1103/PhysRevB.75.075420>.
- [25] G. Gao, S.H. Park, H.S. Kang, A first principles study of NO₂ chemisorption on silicon carbide nanotubes, *Chem. Phys.* 355 (2009) 50–54, <https://doi.org/10.1016/j.chemphys.2008.10.049>.
- [26] G. Guo, F. Wang, H. Sun, D. Zhang, Reactivity of silicon-doped carbon nanotubes toward small gaseous molecules in the atmosphere, *Int. J. Quantum Chem.* 108 (2008) 203–209, <https://doi.org/10.1002/qua.21460>.
- [27] H. Jiang, D. Zhang, R. Wang, Silicon-doped carbon nanotubes: a potential resource for the detection of chlorophenols/chlorophenoxy radicals, *Nanotechnology* 20 (2009), <https://doi.org/10.1088/0957-4484/20/14/145501>.
- [28] D. Kang, X. Yu, M. Ge, F. Xiao, H. Xu, Novel Al-doped carbon nanotubes with adsorption and coagulation promotion for organic pollutant removal, *J. Environ. Sci.* 54 (2017) 1–12, <https://doi.org/10.1016/j.jes.2016.04.022>.
- [29] W. Li, G.-Q. Li, X.-M. Lu, J.-J. Ma, P.-Y. Zeng, Q.-Y. He, Y.-Z. Wang, Strong adsorption of Al-doped carbon nanotubes toward cisplatin, *Chem. Phys. Lett.* 658 (2016) 162–167, <https://doi.org/10.1016/j.cplett.2016.06.040>.
- [30] Q. Li, F. Yuan, C. Yan, J. Zhu, J. Sun, Y. Wang, J. Ren, X. She, Germanium and phosphorus co-doped carbon nanotubes with high electrocatalytic activity for oxygen reduction reaction, *RSC Adv.* 6 (2016) 33205–33211, <https://doi.org/10.1039/c5ra26675k>.
- [31] H. He, C. Yuan, E. Liang, S. Li, Field emission of gallium-doped carbon nanotubes, in: C.X. Cui, Y.L. Li, Z.H. Yuan (Eds.), *Adv. Eng. Mater.* 12 (2010) p. 61+, <https://doi.org/10.4028/www.scientific.net/AMR.535-537.61>. PTS 1-3.
- [32] Y. Li, R. Ahuja, J.A. Larsson, Communication: origin of the difference between carbon nanotube armchair and zigzag ends, *J. Chem. Phys.* 140 (2014), <https://doi.org/10.1063/1.4867744>.
- [33] A.D. Becke, A new mixing of hartree-fock and local density functional theories, *J. Chem. Phys.* 98 (1993) 1372–1377, <https://doi.org/10.1063/1.464304>.
- [34] M.J. Frisch, G.W. Trucks, H.B. Schlegel, G.E. Scuseria, M.A. Robb, J.R. Cheeseman, G. Scalmani, V. Barone, B. Mennucci, G.A. Petersson, H. Nakatsuji, M. Caricato, X. Li, H.P. Hratchian, A.F. Izmaylov, J. Bloino, G. Zheng, J.L. Sonnenberg, M. Hada, M. Ehara, K. Toyota, R. Fukuda, J. Hasegawa, M. Ishida, T. Nakajima, Y. Honda, O. Kitao, H. Nakai, T. Vreven, J.A. Montgomery, J.E. Peralta, F. Ogliaro, M. Bearpark, J.J. Heyd, E. Brothers, K.N. Kudin, V.N. Staroverov, R. Kobayashi, J. Normand, K. Raghavachari, A. Rendell, J.C. Burant, S.S. Iyengar, J. Tomasi, M. Cossi, N. Rega, J.M. Millam, M. Klene, J.E. Knox, J.B. Cross, V. Bakken, C. Adamo, J. Jaramillo, R. Gomperts, R.E. Stratmann, O. Yazyev, A.J. Austin, R. Cammi, C. Pomelli, J.W. Ochterski, R.L. Martin, K. Morokuma, V.G. Zakrzewski, G.A. Voth, P. Salvador, J.J. Dannenberg, S. Dapprich, A.D. Daniels, Farkas, J.B. Foresman, J. V Ortiz, J. Cioslowski, D.J. Fox, Gaussian 09, Revision E.01, Gaussian Inc., Wallingford CT, 2009.
- [35] M. Yoosefian, M. Zahedi, A. Mola, S. Naserian, A DFT comparative study of single and double SO₂ adsorption on Pt-doped and Au-doped single-walled carbon nanotube, *Appl. Surf. Sci.* 349 (2015) 864–869, <https://doi.org/10.1016/j.apsusc.2015.05.088>.
- [36] S.-L. Sun, Y.-Y. Hu, H.-L. Xu, Z.-M. Su, L.-Z. Hao, Probing the linear and nonlinear optical properties of nitrogen-substituted carbon nanotube, *J. Mol. Model.* 18 (2012) 3219–3225, <https://doi.org/10.1007/s00894-011-1334-7>.
- [37] Z. Izakmehri, M. Ardjmand, M.D. Ganji, E. Babanezhad, A. Heydarinasab, Removal of dioxane pollutants from water by using Al-doped single walled carbon nanotubes, *RSC Adv.* 5 (2015) 48124–48132, <https://doi.org/10.1039/c5ra07611k>.
- [38] R. Jawaria, M. Hussain, M. Khalid, M.U. Khan, M.N. Tahir, M.M. Naseer, A.A. Carmo Braga, Z. Shafiq, Synthesis, crystal structure analysis, spectral characterization and nonlinear optical exploration of potent thio-semicarbazones based compounds: a DFT refine experimental study, *Inorg. Chim. Acta* 486 (2019) 162–171, <https://doi.org/10.1016/j.ica.2018.10.035>.
- [39] R.G. Parr, R.G. Pearson, Absolute hardness - companion parameter to absolute electronegativity, *J. Am. Chem. Soc.* 105 (1983) 7512–7516, <https://doi.org/10.1021/ja00364a005>.
- [40] P. Geerlings, F. De Proft, W. Langenaeker, Conceptual density functional theory, *Chem. Rev.* 103 (2003) 1793–1873, <https://doi.org/10.1021/cr990029p>.
- [41] N.M. O'Boyle, A.L. Tenderholt, K.M. Langner, cclib, A library for package-independent computational chemistry algorithms, *J. Comput. Chem.* 29 (2008) 839–845, <https://doi.org/10.1002/jcc.20823>.
- [42] G. Chen, Y. Seki, H. Kimura, S. Sakurai, M. Yumura, K. Hata, D.N. Futaba, Diameter control of single-walled carbon nanotube forests from 1.3–3.0 nm by arc plasma deposition, *Sci. Rep.* 4 (2014), <https://doi.org/10.1038/srep03804>.
- [43] R. Lortz, Q. Zhang, W. Shi, J.T. Ye, C. Qiu, Z. Wang, H. He, P. Sheng, T. Qian, Z. Tang, N. Wang, X. Zhang, J. Wang, C.T. Chan, Superconducting characteristics of 4-(\ A) carbon nanotube{\ extenddash}zeolite composite, *Proc. Natl. Acad. Sci. Unit. States Am.* 106 (2009) 7299–7303, <https://doi.org/10.1073/pnas.0813162106>.
- [44] M.R. Momeni, F.A. Shakib, Stable C₂₀–nSin heterofullerenes (n≤8): a DFT approach, *Chem. Phys. Lett.* 492 (2010) 137–141, <https://doi.org/10.1016/j.cplett.2010.04.051>.
- [45] F. Naderi, M.R. Momeni, F.A. Shakib, Theoretical study of highly doped heterofullerenes evolved from the smallest fullerene cage, *Struct. Chem.* 23 (2012) 1503–1508, <https://doi.org/10.1007/s11224-012-9958-5>.
- [46] C. Shao, J. Xia, J. Zhang, Q. Shao, Effects of B–N co-doping into the ultra-small diameter zigzag single-walled carbon nanotubes: a density functional theory study, *Phys. E Low-dimens. Syst. Nanostruct.* 59 (2014) 88–92, <https://doi.org/10.1016/j.physe.2013.12.023>.
- [47] R. Chegel, Effects of carbon doping on the electronic properties of boron nitride nanotubes: tight binding calculation, *Phys. E Low-dimens. Syst. Nanostruct.* 84 (2016) 223–234, <https://doi.org/10.1016/j.physe.2016.06.003>.
- [48] S. Behzad, R. Chegel, Engineering thermal and electrical properties of B/N doped carbon nanotubes: tight binding approximation, *J. Alloy. Comp.* 792 (2019) 721–731, <https://doi.org/10.1016/j.jallcom.2019.03.381>.
- [49] R. Ghoreishi, M. Kia, Chemical reactivity and adsorption properties of pro-carbazine anti-cancer drug on gallium-doped nanotubes: a quantum chemical study, *J. Mol. Model.* 25 (2019), <https://doi.org/10.1007/s00894-018-3914-2>.
- [50] J.H. Warner, F. Schaeffel, G. Zhong, M.H. Ruemmel, B. Buechner, J. Robertson, G.A.D. Briggs, Investigating the diameter-dependent stability of single-walled carbon nanotubes, *ACS Nano* 3 (2009) 1557–1563, <https://doi.org/10.1021/nn900362a>.
- [51] F. Xu, L.X. Sun, J. Zhang, Y.N. Qi, L.N. Yang, H.Y. Ru, C.Y. Wang, X. Meng, X.F. Lan, Q.Z. Jiao, F.L. Huang, Thermal stability of carbon nanotubes, *J. Therm. Anal. Calorim.* 102 (2010) 785–791, <https://doi.org/10.1007/s10973-010-0793-x>.
- [52] F. Yu, M. Yang, F. Li, C. Su, B. Ma, Z. Yuan, J. Chen, J. Ma, The growth mechanism of single-walled carbon nanotubes with a controlled diameter, *Phys. E Low-dimens. Syst. Nanostruct.* 44 (2012) 2032–2040, <https://doi.org/10.1016/j.physe.2012.06.007>.
- [53] M. Kurban, Electronic structure, optical and structural properties of Si, Ni, B and N-doped a carbon nanotube: DFT study, *Optik* 172 (2018) 295–301, <https://doi.org/10.1016/j.ijleo.2018.07.028>.
- [54] J.R. Sanchez-Valencia, T. Dienel, O. Groening, I. Shorubalko, A. Mueller, M. Jansen, K. Amsharov, P. Ruffieux, R. Fasel, Controlled synthesis of single-chirality carbon nanotubes, *Nature* 512 (2014) 61+, <https://doi.org/10.1038/nature13607>.
- [55] T. Ando, Theory of electronic states and transport in carbon nanotubes, *J. Phys. Soc. Japan* 74 (2005) 777–817, <https://doi.org/10.1143/JPSJ.74.777>.
- [56] C. Zhao, X. Zhou, S. Xie, H. Wei, J. Chen, X. Chen, C. Chen, DFT study of electronic structure and properties of N, Si and Pd-doped carbon nanotubes, *Ceram. Int.* 44 (2018) 21027–21033, <https://doi.org/10.1016/j.ceramint.2018.08.138>.
- [57] S.S. Yu, Q.B. Wen, W.T. Zheng, Q. Jiang, Effects of doping nitrogen atoms on the structure and electronic properties of zigzag single-walled carbon nanotubes through first-principles calculations, *Nanotechnology* 18 (2007), <https://doi.org/10.1088/0957-4484/18/16/165702>.
- [58] R.G. Pearson, The principle of maximum hardness, *Acc. Chem. Res.* 26 (1993) 250–255, <https://doi.org/10.1021/ar00029a004>.
- [59] N. Sundaraganesan, E. Kavitha, S. Sebastian, J.P. Cornard, M. Martel, Experimental FFIR, FT-IR (gas phase), FT-Raman and NMR spectra, hyperpolarizability studies and DFT calculations of 3,5-dimethylpyrazole, *Spectrochim. Acta Part A-Molecular Biomol. Spectrosc.* 74 (2009) 788–797, <https://doi.org/10.1016/j.saa.2009.08.019>.
- [60] D. Sajan, H. Joe, V.S. Jayakumar, J. Zaleski, Structural and electronic contributions to hyperpolarizability in methyl p-hydroxy benzoate, *J. Mol. Struct.* 785 (2006) 43–53, <https://doi.org/10.1016/j.molstruc.2005.09.041>.
- [61] S.N. Margara, N. Sekar, Nonlinear optical properties of curcumin: solvatochromism-based approach and computational study, *Mol. Phys.* 114 (2016) 1867–1879, <https://doi.org/10.1080/00268976.2016.1161248>.
- [62] S. Katariya, L. Rhyman, I.A. Alswaidan, P. Ramasami, N. Sekar, Triphenylamine-based fluorescent styryl dyes: DFT, TD-DFT and non-linear optical property study, *J. Fluoresc.* 27 (2017) 993–1007, <https://doi.org/10.1007/s10895-017-2034-1>.
- [63] M.M.L. Kadam, D. Patil, N. Sekar, Carbazole based NLOphoric styryl dyes-synthesis and study of photophysical properties by solvatochromism and viscosity sensitivity, *J. Lumin.* 202 (2018) 212–224, <https://doi.org/10.1016/j.jlumin.2018.05.059>.
- [64] M.D.H. Bhuiyan, M. Ashraf, A. Teshome, G.J. Gainsford, A.J. Kay, I. Asselberghs, K. Clays, Synthesis, linear & non linear optical (NLO) properties of some indoline based chromophores, *Dyes Pigments* 89 (2011) 177–187, <https://doi.org/10.1016/j.dyepig.2010.10.010>.
- [65] N.M. Ravindra, S. Auluck, V.K. Srivastava, On the penn gap in semiconductors, *Phys. Status Solidi B* 93 (1979) K155–K160, <https://doi.org/10.1002/psb.2220930257>.